PHYSICAL REVIEW D **85,** 034012 (2012)

Hadron interaction with heavy quarkonia

I. V. Danilkin*

Gesellschaft fur Schwerionenforschung (GSI) Planck Str. 1, 64291 Darmstadt, Germany, Institute of Theoretical and Experimental Physics, Moscow, Russia

V. D. Orlovsky† and Yu. A. Simonov‡

Institute of Theoretical and Experimental Physics, Moscow, Russia

(Received 17 October 2011; published 7 February 2012)

Dynamics of hadro-quarkonium system is formulated, based on the channel coupling of a light hadron (h) and heavy quarkonium ($Q\bar{Q}$) to intermediate open-flavor heavy-light mesons ($Q\bar{q}$, $\bar{Q}q$). The resulting effective interaction is defined by overlap integrals of meson wave functions and ($hq\bar{q}$) coupling, where h is π, ρ, ω, ϕ, without fitting parameters. Equations for hadro-quarkonium amplitudes and resonance positions are written explicitly, and numerically calculated for the special case of $\pi\Upsilon(nS)$ ($n = 1, 2, 3$). It is also shown that the recently observed by Belle two peaks $Z_b(10610)$ and $Z_b(10650)$ are in agreement with the proposed theory. It is demonstrated, that theory predicts peaks at the BB^*, B^*B^* thresholds in all available $\pi\Upsilon(nS)$ channels. Analytic nature of these peaks is investigated, and shown to be due to a common multichannel resonance poles close to the BB^*, B^*B^* thresholds. The general mechanism of these hadro-quarkonium resonances does not assume any molecular or four-quark (tetraquark) dynamics.

DOI: 10.1103/PhysRevD.85.034012 PACS numbers: 14.40.Nd, 13.25.Gv

I. INTRODUCTION

It was found in experiment [1–4] that resonances may appear in the system of a hadron and heavy quarkonium, which may be called hadro-quarkonium, see [5] for a review. On theoretical side, the prevalent approaches associate hadro-quarkonia with molecular or four-quark ($4q$) states [6–16]. In the first case, hadro-quarkonia are weakly bound states of two heavy-light mesons of the closest threshold with interaction tuned to produce loosely bound or virtual states, and in the $4q$ states thresholds cannot be easily connected with $4q$. However, it will be argued that channel coupling (CC) near thresholds may play the dominant role in hadro-quarkonium dynamics, as was shown for heavy quarkonia in our previous papers [17,18].[1] It was shown there that strong CC, calculated basically without fitting parameters, shifts the 2^3P_1 ($c\bar{c}$) pole exactly to the $D\bar{D}^*$ threshold. In this way, the $X(3872)$ phenomenon was explained using only one parameter M_ω, which was fixed in previous studies [24–27] and universal input: the string tension σ, the current (pole) quark masses, and the strong coupling $\alpha_s(q)$. Recently M_ω was found from the first principles in QCD [28]. It was shown there, that M_ω can be calculated as the matrix element of the operator σr, where σ is the string tension and r is the length of the string. The decay width of $\psi(3770)$ is reproduced in this way and corresponds to $M_\omega \approx 0.8$ GeV. Our starting point is the first principle derivation of the CC interaction of standard heavy quarkonia with open flavor channels, using strong decay theory [28]. Similarly, in the phenomenon of $X(3872)$, the systems $\omega J/\psi$ and $\rho J/\psi$ may take part with the thresholds near those of ($D\bar{D}^*$ + H.c.) states. In the same way, additional pions in the decay vertex appear with the only extra factor in the denominator $f_\pi = 93$ MeV. As will be shown below, the strong interaction of pions with $Y(nS)$ mesons produces charged Z-type resonances. Recently in a series of papers [24,25], the CC methods have been successfully applied to the transitions in systems, containing heavy quarkonia and pions, or η meson and in this way the main features of experimental pionic spectra in reactions $X' \to X\pi\pi$ were explained together with kaonic and η-meson final states [26,27]. Below, we extend the formalism of channel coupling (CC) developed in [17,18] to the case of a hadron $h = \pi, \phi, \eta, \rho, \omega, \ldots$ interacting with the $Q\bar{Q}$ state.

We study the interaction and possible poles of hadro-quarkonium amplitudes in the formalism of [17]. We assume that the most important interaction in hadro-quarkonium is due to intermediate states of heavy-light mesons $(Q\bar{q})(\bar{Q}q)$ (e.g. DD, DD^*, D^*D^*, D_sD_s, ... in case of hadro-charmonium). Therefore, one should sum up the whole series of bubbles, consisting of hadro-quarkonia and heavy-light mesons, as shown in Fig. 1. To find poles in amplitudes, one can start and finish with any state, since poles belong to all channels, i.e. $h(Q\bar{Q})$ and $(Q\bar{q})(\bar{Q}q)$. We shall formally study the amplitudes for the transition of two heavy-light mesons again into the same or other pair of heavy-light mesons.

It is important to stress that in our mechanism of hadro-quarkonium resonances there is no direct interaction

*danilkin@itep.ru
†orlovskii@itep.ru
‡simonov@itep.ru

[1]Similar in spirit, but different technically, the so-called rescattering model was developed and applied, in particular, to dipion transitions in bottomonia in [19–23]

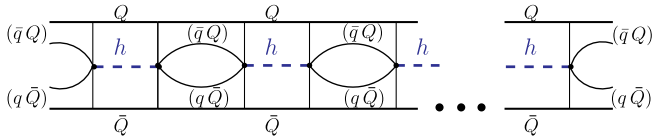

FIG. 1 (color online). The chain of transitions of hadro-quarkonia ($h + Q\bar{Q}$) and pair of heavy-light mesons $(Q\bar{q}) \times (\bar{Q}q)$. h denotes light hadrons ($h = \pi, \phi, \ldots$).

neither in the hadron-quarkonium channel, nor in the channel of two heavy-light mesons. The only interaction, which generates resonance poles, is the CC interaction, transforming hadro-quarkonium system into double heavy-light system. Therefore hadro-quarkonium resonances, predicted in our theory, are a clear example of CC resonances, introduced and calculated earlier in [29]. We show below that direct molecular resonances of BB^* (if any) are displaced and split in hadro-quarkonium in different hadro-quarkonium channels.

To find the poles, we can use the so-called Weinberg eigenvalue method (WEM), discussed in detail in [17]. It allows us to define not only poles, but also resonance wave functions and was successfully applied in [17] to charmonia states and, in particular, to $X(3872)$, in a situation of strongly coupled channels. It was shown in [17,18] that $X(3872)$ is due to bare $n = 2^3P_1$ resonance, shifted exactly to the D^0D^{*0} threshold by CC and the detailed experimental form was reproduced in [17,18] with a tiny cusp at the D^+D^- threshold and no other bumps. No connection to $\rho J/\psi$ and $\omega J/\psi$ channels was taken into account in [17,18], assuming the corresponding partial widths to be generally small, and here we establish formalism for these channels, and $\phi J/\psi$, which allows to find out, whether the CC interaction in these cases is strong enough to produce poles. The situation with the $\omega J/\psi$ channel is especially interesting since it contains the resonance of its own, $Y(3940)$ [1], but in addition the decay $X(3872) \to \omega J/\psi$, found in [30], (see [31] for a recent review) suggests that the whole CC system for $X(3872)$ should contain channels $2^3P_1(c\bar{c})$, DD^*, $\omega J/\psi$ and $\rho J/\psi$. The CC analysis of this system in another framework (resonance-spectrum method) [32], was done recently in [33].

A special case of hadro-quarkonium is the pion-quarkonium system, where the CC interaction vertex is proportional to $1/f_\pi$ and numerically large, which might support the appearance of $\pi(Q\bar{Q})$ resonances. Below we shall study specifically the case of $\pi\pi$ transitions in the $\Upsilon(nS)$ states, where these resonances appear in the final states $\Upsilon(n'S)\pi\pi$.

The plan of the paper is as follows. In Sec. II, some basic equations of WEM in the hadro-quarkonium case are written, and in Sec. III those are exploited to write down exact equation for the possible poles in the general case of three sectors. In Sec. IV, the special case of the pion-quarkonium system is treated in detail and $(\pi\Upsilon(nS))$ are found for $n = 1, 2, 3$. In Sec. V, results of calculations are given, and Sec. VI contains conclusions, comparison of molecular and CC dynamics and outlook. Two appendices are devoted to detailed derivation of decay transition kernel and the form of wave functions.

II. DYNAMICS OF STRONG CHANNEL COUPLING FOR HADRO-QUARKONIUM

We consider two strongly interacting sectors: sector I with a heavy quarkonium state $(Q\bar{Q})$ plus hadron $h = \pi$, ω, ρ, η, ϕ etc., and sector II, consisting of two heavy-light mesons $(Q\bar{q})(\bar{Q}q)$; in case of hadro-charmonium, it could be $D\bar{D}$, $D\bar{D}^*$, $D^*\bar{D}^*$, $D\bar{D}_1$, $D_s\bar{D}_s$ etc.

It is important that we neglect interaction between any white objects, considering the limit of large N_c. This means that in our treatment there is no direct interaction between hadron and heavy quarkonium, as well as between heavy-light mesons. Justification of this approximation can be found in the fact known from NN interaction, that the main part of long-range forces between white objects comes from the exchange of one pion or a pair of correlated pions, which in case of a deutron yields a small binding energy. However, heavy quarks in heavy-light mesons do not contribute in this process and hence one-pion exchange in the system of two heavy-light mesons should be much smaller, that in the NN system. This is also supported by the fact that ΛN, ΣN and $\Lambda\Lambda$, $\Sigma\Sigma$ interactions are relatively weaker, that the NN interaction. Therefore from our point of view in the molecular models of exotic charmonia one should take into account that much stronger attraction near the threshold occurs due to CC interaction between sectors I and II. One more support of this comes from our recent study of $X(3872)$ dynamics in [17,18], where we have shown that CC alone strongly shifts 2^3P_1 $c\bar{c}$ level by $\sim$60 MeV to the D^0D^{*0} threshold at 3872 MeV.

As was shown in [17], to study dynamics of CC in our case, one can reduce problem to the one-channel case, where another channel enters via the CC interaction V_{aba} and a, b refer to sectors I, II, respectively. If one is interested only in the possibility of bound states or resonances due to CC, one can start with any channel, and we shall work mostly in channel II and consider the amplitudes shown in Fig. 1 which are generated by the interaction V_{212}. This interaction in the formalism developed in [17] can be written in momentum space as the amplitude of the loop diagram, shown in Fig. 2, with hadron (h) and quarkonium $(Q\bar{Q})$ in the n-th state

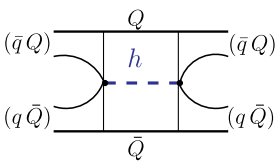

FIG. 2 (color online). The diagram of the hadron interaction $V^{(h)}_{n_2n_3;n_2'n_3'}$.

$$V^{(h)}_{n_2n_3,n_2'n_3'}(\mathbf{p},\mathbf{p}',E)=\sum_n\int\frac{d^3\mathbf{k}}{(2\pi)^3}\times\frac{J^{(h)}_{nn_2n_3}(\mathbf{p},\mathbf{k})J^{(h)}_{nn_2'n_3'}(\mathbf{p}',-\mathbf{k})}{2\omega_h(\mathbf{k})(E-E_n(\mathbf{k})-\omega_h(\mathbf{k}))},\tag{1}$$

with $E_n(\mathbf{p})=\sqrt{\mathbf{p}^2+M_n^2}$, where M_n is the position of the n-th bare quarkonium $(Q\bar{Q})$ state. Indices n_2n_3, $n_2'n_3'$ denote in- and out- quantum states of heavy-light masons, the hadron energy is $\omega_h(\mathbf{k})=\sqrt{\mathbf{k}^2+m_h^2}$, and the overlap matrix elements $J^{(h)}_{nn_2n_3}(\mathbf{p},\mathbf{k})$ define the probability amplitude for the transition of two heavy-light mesons $(Q\bar{q})_{n_2}$, $(\bar{Q}q)_{n_3}$ with quantum numbers n_2, n_3 to quarkonium n-th state $(Q\bar{Q})_n$ plus hadron h. One can derive $J^{(h)}_{nn_2n_3}$ as a matrix element of a hadron emission operator between wave functions of quarkonium and two heavy-light mesons

$$\begin{aligned}J^{(h)}_{nn_2n_3}(\mathbf{p},\mathbf{k})&=\frac{1}{\sqrt{N_c}}\int\bar{y}^{(h)}_{123}\Psi^{(n)}_{Q\bar{Q}}(\mathbf{u}-\mathbf{v})e^{i\mathbf{pr}+i\mathbf{kx}}\psi_{n_2}(\mathbf{u}-\mathbf{x})\\&\times\psi_{n_3}(\mathbf{x}-\mathbf{v})d^3\mathbf{x}d^3(\mathbf{u}-\mathbf{v})\\&=\frac{1}{\sqrt{N_c}}\int\frac{d^3q}{(2\pi)^3}\bar{y}^{(h)}_{123}\Psi^{(n)}_{Q\bar{Q}}\left(c\mathbf{p}-\frac{\mathbf{k}}{2}+\mathbf{q}\right)\\&\times\psi^{(n_2)}_{Q\bar{q}}(\mathbf{q})\psi^{(n_3)}_{\bar{Q}q}(\mathbf{q}-\mathbf{k}),\end{aligned}\tag{2}$$

where N_c is the number of colors, $\mathbf{r}=c(\mathbf{u}-\mathbf{v})$, $c=\frac{\omega_Q}{\omega_Q+\omega_q}$. We point that the w.f $\Psi^{(n)}_{Q\bar{Q}}$, $\psi^{(n_2)}_{Q\bar{q}}$, $\psi^{(n_3)}_{\bar{Q}q}$ in (8) are no longer full wave function (w.f.) of mesons, but the radial part $R^{(n)}_{Q\bar{Q}}$, $R^{(n_2)}_{Q\bar{q}}$, $R^{(n_3)}_{\bar{Q}q}$ divided by $\sqrt{4\pi}$, while the angular part of the w.f. is accounted for in the factor $\bar{y}^{(h)}_{123}$. This transition kernel $\bar{y}^{(h)}_{123}$ contains a coupling constant g_h of hadron with quark pair $(q\bar{q})$, entering the hadron string-breaking $(hq\bar{q})$ Lagrangian for light vector mesons

$$\mathcal{L}_h=\int\bar{\psi}g_h\hat{e}\psi\frac{e^{ikx}d^4x}{\sqrt{2\omega_hV_3}},\tag{3}$$

and another part, which comes from the Dirac trace of γ matrices corresponding to the vertices in state $(Q\bar{Q})_n$ and $(Q\bar{q})_{n_2}$, $(\bar{Q}q)_{n_3}$. In Eq. (3) V_3 is the normalization volume and $\hat{e}=\gamma^\mu e_\mu$.

To obtain the full vertex $\bar{y}^{(h)}_{123}$ in (2), one can use either the (4×4) form given in [24,25] or else the (2×2) form for wave functions and vertices, introduced in [17], Appendix B. Exact expressions for $\bar{y}^{(h)}_{123}$ are given in Appendix A for the convenience of the reader. In this way for the n_1 state of quarkonia and vector hadron, one can write similarly to (B3)

$$\bar{y}^{(h)}_{123}=\mathrm{tr}\{\Gamma^{(n_1)}_{\mathrm{red}}\Gamma^{(n_2)}_{\mathrm{red}}(\mathbf{e}\boldsymbol{\sigma})g_h\Gamma^{(n_3)}_{\mathrm{red}}\}\tag{4}$$

and

$$\begin{aligned}\Gamma^{(n)}_{\mathrm{red}}(D)&=\frac{1}{\sqrt{2}},\\\Gamma^{(n)}_{\mathrm{red}}(D^*)&=\frac{\sigma_k}{\sqrt{2}},\\\Gamma^{(n)}_{\mathrm{red}}(1^{--}(Q\bar{Q}))&=\frac{\sigma_i}{\sqrt{2}},\end{aligned}\tag{5}$$

where σ_i are the Pauli matrices. Therefore, in the case $1^{--}(Q\bar{Q})+h\to D\bar{D}^*$, one obtains

$$\bar{y}^{(h)}_{123}=ig_he_j\epsilon_{ijk}\tag{6}$$

where e is the polarization vector of hadron and ϵ_{ijk} is the Levi-Civita symbol.

For Nambu-Goldstone bosons (π,K,η) the transition kernel was obtained in a different way in [24]. Indeed, pions accompany string breaking, yielding a coefficient $\frac{M_\omega}{f_\pi}\gamma_5$ instead of g_h in (3), where M_ω is calculated via string tension σ in [28], $M_\omega=0.8$ GeV. This is used in Sec. IV below; details are given in Appendices A and B.

To define possible resonance position and wave function it is convenient to use the Weinberg Eigenvalue Method, which was extended to the case of coupled channel problem in [17]. The corresponding equation for eigenfunction $\psi^{(\nu)}(\mathbf{r},E)$ and eigenvalue $\eta_\nu(E)$ can be written as

$$H_0\psi^{(\nu)}(\mathbf{r},E)+\frac{1}{\eta_\nu(E)}\int V_{212}(\mathbf{r},\mathbf{r}',E)\psi^{(\nu)}(\mathbf{r}',E)d^3\mathbf{r}'=E\psi^{(\nu)}(\mathbf{r},E),\tag{7}$$

where H_0 is the one-channel Hamiltonian in sector II with the neglected in the first approximation a direct interaction between two color singlet mesons. The boundary conditions are

$$\psi^{(\nu)}(r\to\infty,E)\sim\frac{\exp(ikr)}{r},\qquad\psi^{(\nu)}(0,E)=\mathrm{const},$$

where k is the c.m. momentum of mesons defined by the condition $E=\sqrt{k^2+M_{n_2}}+\sqrt{k^2+M_{n_3}}$. Index ν labels the discrete eigenvalues and eigenvectors. In the momentum space, one can write

$$\begin{aligned}\psi^{(\nu)}_{n_2n_3}(\mathbf{p},E)&=-\frac{1}{\eta_\nu(E)}\sum_{n_2'n_3'}\int\frac{d^3\mathbf{p}'}{(2\pi)^3}G^{(0)}_{n_2n_3}(\mathbf{p})V^{(h)}_{n_2n_3,n_2'n_3'}(\mathbf{p},\mathbf{p}',E)\\&\times\psi^{(\nu)}_{n_2'n_3'}(\mathbf{p}')\\G^{(0)}_{n_2n_3}(\mathbf{p},E)&=\frac{1}{E_{n_2}(\mathbf{p})+E_{n_3}(\mathbf{p})-E}.\end{aligned}\tag{8}$$

At this point, one realizes that Eq. (8) can be seriously simplified using the structure of the overlap integrals in (2). Indeed, it was shown in [24,25] that wave functions of heavy-light mesons D, D^* (B,B^*) can be represented by the Gaussian functions with accuracy of the order of a few

percent. In this case, the integral in (2) factorizes (see Eq. (21) in [25])

$$J^{(h)}_{nn_2n_3}(\mathbf{p},\mathbf{k}) \equiv \frac{1}{\sqrt{N_c}}\varphi^{(h)}_{n_2n_3}(\mathbf{k})\chi^{(h)}_{nn_2n_3}(\mathbf{p}). \tag{9}$$

Moreover, it appears that $\varphi^{(h)}_{n_2n_3}(\mathbf{k})$ are almost identical for the first two states of heavy-light mesons (e.g. B, B^*) and are very close for the next two states (e.g. B_s, B_s^*), hence we simplify $\varphi^{(h)}_{n_2n_3}$ to $\varphi^{(h)}$.

As one can see in (1), the integral on the right-hand side (rhs) also factorizes, when (9) is used, and one can write

$$V^{(h)}_{n_2n_3,n_2'n_3'}(\mathbf{p},\mathbf{p}',E) = -\sum_n \frac{1}{N_c}\chi^{(h)}_{nn_2n_3}(\mathbf{p})\chi^{(h)}_{nn_2'n_3'}(\mathbf{p}')K_n(E), \tag{10}$$

where notation is used

$$K_n(E) = \int \frac{d^3\mathbf{k}}{(2\pi)^3}\frac{\varphi^{(h)}(\mathbf{k})\varphi^{(h)}(-\mathbf{k})}{2\omega_h(\mathbf{k})(E_n(\mathbf{k})+\omega_h(\mathbf{k})-E)}. \tag{11}$$

Insertion of (10) in (8) immediately yields

$$\psi^{(\nu)}_{n_2n_3}(\mathbf{p},E) = \frac{1}{N_c}\frac{G^{(0)}_{n_2n_3}(\mathbf{p},E)}{\eta_\nu(E)}\sum_n K_n(E)\chi^{(h)}_{nn_2n_3}(\mathbf{p}) \times \sum_{n_2'n_3'}\int\frac{d^3\mathbf{p}'}{(2\pi)^3}\chi^{(h)}_{nn_2'n_3'}(\mathbf{p}')\psi^{(\nu)}_{n_2'n_3'}(\mathbf{p}',E), \tag{12}$$

which finally leads to a system of algebraic equations

$$\Lambda^{(\nu)}_{n'}(E) = \frac{1}{\eta_\nu(E)}\sum_n \zeta_{n'n}(E)K_n(E)\Lambda^{(\nu)}_n(E),$$
$$\Lambda^{(\nu)}_n(E) \equiv \sum_{n_2n_3}\int\frac{d^3\mathbf{p}}{(2\pi)^3}\chi^{(h)}_{nn_2n_3}(\mathbf{p})\psi^{(\nu)}_{n_2n_3}(\mathbf{p},E), \tag{13}$$

where we have defined in (13)

$$\zeta_{nn'}(E) = \frac{1}{N_c}\sum_{n_2n_3}\int\frac{d^3\mathbf{p}}{(2\pi)^3}G^{(0)}_{n_2n_3}(\mathbf{p},E)\chi^{(h)}_{nn_2n_3}(\mathbf{p})\chi^{(h)}_{n'n_2n_3}(\mathbf{p}). \tag{14}$$

So, we obtain

$$\det[\eta_\nu(E)\delta_{nn'} - K_n(E)\zeta_{nn'}(E)] = 0 \tag{15}$$

and one can look for poles E_p, setting $\eta_\nu(E=E_p)=1$.

Equivalently, one can define amplitude in the sector I, $h+(Q\bar{Q})$, in which case the interaction "potential" V_{121} assumes the form

$$V^{(h)}_{nn'}(\mathbf{k},\mathbf{k}',E) = \sum_{n_2n_3}\int\frac{d^3\mathbf{p}}{(2\pi)^3}\frac{J^{(h)}_{nn_2n_3}(\mathbf{p},\mathbf{k})J^{(h)}_{n'n_2n_3}(\mathbf{p},\mathbf{k}')}{E-H_0^{(n_2n_3)}(\mathbf{p})} \tag{16}$$

and the WEM equation in sector I is

$$\psi^{(\nu)}_n(\mathbf{k},E) = -\int\frac{d^3\mathbf{k}'}{(2\pi)^3 2\omega(\mathbf{k}')}G^{(0)}_n(\mathbf{k},E) \times \frac{V^{(h)}_{nn'}(\mathbf{k},\mathbf{k}',E)}{\eta_\nu(E)}\psi^{(\nu)}_{n'}(\mathbf{k}',E). \tag{17}$$

One can see from (16) that $V^{(h)}_{121}$ is attractive and real for E below the $D\bar{D}(D\bar{D}^*)$ threshold, and $G^{(0)}_n$ is

$$G^{(0)}_n(\mathbf{k},E) = \frac{1}{H_0(\mathbf{k})-E} = \frac{1}{E_n(\mathbf{k})+\omega_h(\mathbf{k})-E}. \tag{18}$$

The total Green's function in sector I has the form (see [17] for discussion and details)

$$G^{(\mathrm{I})}(1,2;E) = \sum_\nu \frac{\psi^{(\nu)}_n(1,E)\psi^{+(\nu)}_n(2,E)}{1-\eta_\nu(E)} \tag{19}$$

and near the resonance $\eta_\nu(E)$ has the form

$$\eta_\nu(E) = 1 + \eta_\nu'\left(E_0 - \frac{i\Gamma}{2}\right)\left(E - E_0 + \frac{i\Gamma}{2}\right) + \ldots \tag{20}$$

where E_p was replaced by $E_0 - \frac{i\Gamma}{2}$. Finally, one can define the t-matrix

$$t = \hat{V} - \hat{V}G\hat{V}, \tag{21}$$

which in the WEM can be written as

$$t(\mathbf{k},\mathbf{k}',E) = -\sum_\nu \frac{\eta_\nu(E)a_\nu(\mathbf{k},E)a_\nu(\mathbf{k}',E)}{1-\eta_\nu(E)} \tag{22}$$

where

$$a_\nu(\mathbf{k},E) = (H_0(\mathbf{k})-E)\psi^{(\nu)}_n(\mathbf{k},E). \tag{23}$$

III. A GENERAL CASE OF THREE COUPLED SECTORS

Until now, only the connection of given channel $h+(Q\bar{Q})_n$ to $(Q\bar{q})(\bar{Q}q)$ was considered. A more interesting situation can occur when one adds also excited channels of $(Q\bar{Q})_{n'}$. An example of the physical situation of this kind is given by the $2^3P_1(c\bar{c})$ state connected to $\omega J/\psi$ via the DD^* channel. Hence, in this case one has to consider three sectors: as before sectors I and II refer to $h(Q\bar{Q})_n$ and $(Q\bar{q})(\bar{Q}q)$, respectively, and sector III refers to $(Q\bar{Q})_{n'}$ states. One again writes the equation for the wave function in sector II as in Eq. (8), but the interaction $V_{n_2n_3,n_2'n_3'}$ now consists of two terms:

$$V_{n_2n_3,n_2'n_3'}(\mathbf{p},\mathbf{p}',E) = V^{(h)}_{n_2n_3,n_2'n_3'}(\mathbf{p},\mathbf{p}',E) + V^{(Q\bar{Q})}_{n_2n_3,n_2'n_3'}(\mathbf{p},\mathbf{p}',E) \tag{24}$$

where we add to the potential $V^{(h)}$ in Eq. (1) another kernel, $V^{(Q\bar{Q})}$ of the following form (cf Eq. (26) of [17]):

$$V^{(Q\bar{Q})}_{n_2n_3,n_2'n_3'}(\mathbf{p},\mathbf{p}',E)=\sum_n \frac{J^+_{nn_2n_3}(\mathbf{p})J_{nn_2'n_3'}(\mathbf{p}')}{E-M_n}. \quad (25)$$

Here, $J(\mathbf{p})$ is obtained from $J^{(h)}(\mathbf{p},\mathbf{k})$ putting $\mathbf{k}=0$ and replacing $\bar{y}^{(h)}_{123}$ by $M_\omega \bar{y}_{123}$, where $\bar{y}_{123}$ is given in [17] for different states, and M_ω is a fixed parameter for all charmonia and bottomonia states used in [17–26], $M_\omega = 0.8$ GeV, in actual calculations one reduces the fully relativistic vertex $M_\omega \bar{y}_{123}$ to the two-component spinor form, convenient for nonrelativistic form of participating wave-functions $M_\omega \bar{y}_{123} = \gamma \bar{y}^{red}_{123}$, and $\gamma = 1.4$, see appendix C of [17] for details.

The resulting equation for $\eta_\nu(E)$ has the same form as in (13), but now Λ_n and K_n are columns and ζ is a matrix in n and n' indices. Fixing n' and denoting a single channel $n_2n_3 = n_2'n_3' \equiv 1$, one arrives at the equation

$$\det\begin{pmatrix} 1-\frac{1}{\eta_\nu}\zeta_{11}K_1 & -\frac{\zeta_{12}}{\eta_\nu(M_{n'}-E)} \\ -\frac{1}{\eta_\nu}\zeta_{21}K_1 & 1-\frac{\zeta_{22}}{\eta_\nu(M_{n'}-E)}\end{pmatrix}=0, \quad (26)$$

where

$$\zeta_{12}=\zeta_{21}\equiv\int\frac{d^3p}{(2\pi)^3}G^{(0)}_{n_2n_3}(\mathbf{p},E)\chi_{nn_2n_3}(\mathbf{p})J_{n'n_2n_3}(\mathbf{p})$$
$$\zeta_{22}\equiv\sum_{n_2n_3}\int\frac{d^3\mathbf{p}}{(2\pi)^3}G^{(0)}_{n_2n_3}(\mathbf{p},E)J^2_{n'n_2n_3}(\mathbf{p}). \quad (27)$$

The solution of Eq. (26) for $\eta_\nu(E=E_p)=1$ gives the pole positions E_p. In particular, one can derive how the original $(Q\bar{Q})$ pole is shifted due to two effects: 1) CC to the sector II of two heavy-light states $(Q\bar{q})(\bar{Q}q)$ 2) CC due to the hadro-quarkonium states—sector I.

It is clear in (26) that the resulting $\eta_\nu(E)$ contains threshold singularities from sectors II and I and the pole at M_n in the limit of small CC. In the spirit of calculations in [18] and using (22), one can define the probability of transition from sector I to sector II as the absorptive part of t (22) due to sector II. It yields

$$\sigma_{\mathrm{I\,II}}\sim\frac{\frac{1}{2i}\Delta_{\mathrm{II}}\eta_\nu(E)}{|1-\eta_\nu(E)|^2}, \quad (28)$$

where $\Delta_{\mathrm{II}}=\eta_\nu(E+i0)-\eta_\nu(E-i0)$ is the discontinuity along the right hand cut.

The total width Γ of the resonance originating from the state $(Q\bar{Q})_{n'}$ in sector III is obtained from the expansion (20) for small Γ, and from the position of the pole E_p in the equation $\eta_\nu(E_p)=1$, where η_ν is found from (26), for arbitrary γ. The partial widths of the resonance, originating from sector III, corresponding to channels in sectors I and II are proportional to absorptive parts of $\eta_\nu(E)$ on the cuts, starting from thresholds of sectors I and II. The concrete examples of $X(3872)$ connected to $\omega J/\psi$ and $\rho J/\psi$ states will be given elsewhere.

IV. PION-QUARKONIUM RESONANCES

As a specific example of the general formalism in Sec. II, we consider here the pion interaction with heavy quarkonium. To simplify matters, we shall not use WEM in this section, writing all expressions in standard form since we shall not use the notion of resonance wave function for pion quarkonium. The corresponding interaction term $V^{(\pi)}_{n_2n_3,n_2'n_3'}(\mathbf{p},\mathbf{p}',E)$ is given in (1), while $J^{(\pi)}_{nn_2n_3}$ is defined in (2). However, now in contrast to the vector hadron case of (6), one has instead for pion emission the same vertex, which was derived in [17,24,25]. For DD^* or BB^*, one has

$$\bar{y}^{(\pi)}_{123^*}=\frac{M_\omega}{f_\pi}\frac{i\delta_{ik}}{\sqrt{2}}, \quad (29)$$

while for $D^*D^*(B^*B^*)$ one obtains

$$\bar{y}^{(\pi)}_{12^*3^*}=-\frac{M_\omega}{f_\pi}\frac{e_{ikl}}{\sqrt{2}}. \quad (30)$$

Note that indices i, k, l refer to the polarization states of initial and two final vector mesons. Also, the shorthand notation DD^* implies $\frac{1}{\sqrt{2}}(D\bar{D}^*\pm D^*\bar{D})_{\mathrm{I}}$ for the isospin I state. Finally, as in (3) and (6), the factor $\frac{1}{\sqrt{2\omega V_3}}$ is taken into account in the pion phase space integral over $\frac{d^3\mathbf{k}}{(2\pi)^3}$.

With these s-wave-type kernels (29) and (30) and SHO wavefunctions in (2), one can write the factorized form for $J^{(\pi)}_{nn_2n_3}$

$$J^{(\pi)}_{nn_2n_3}(\mathbf{p},\mathbf{k})=\frac{1}{\sqrt{N_c}}\varphi^{(\pi)}_{n_2n_3}(\mathbf{k})\chi_{nn_2n_3}(\mathbf{p}), \quad (31)$$

where

$$\varphi^{(\pi)}_{n_2n_3}(\mathbf{k})=e^{-(\mathbf{k}^2/4\beta_2^2)},$$
$$\chi_{nn_2n_3}(\mathbf{p})=\bar{y}^{(\pi)}_{123}e^{-((c\mathbf{p})^2/\Delta_n)}I_{nn_2n_3}(c\mathbf{p}) \quad (32)$$

and $I_{nn_2n_3}(\mathbf{p})$ for SHO functions for heavy-light mesons with $n_2=n_3=1$ (which gives 95% accuracy for B, B^* and D, D^* mesons [17,24,25]) is

$$I_{n_{11}}(\mathbf{p})=2\tilde{c}_n(-)^{n-1}\frac{(2n-1)!}{(n-1)!}\Phi\left(-(n-1),\frac{3}{2},\mathbf{f}^2\right)\times\frac{y^{n-1}}{(2\sqrt{\pi})^3}\left(\frac{2\beta_1^2\beta_2^2}{\Delta_n}\right)^{3/2} \quad (33)$$

where all constants are defined via SHO parameters of wave functions, participating in the overlap integral (2), see Appendix B.

We note that $\varphi^{(\pi)}_{n_2n_3}(\mathbf{k})\equiv\varphi(\mathbf{k})$ with a good accuracy does not depend on n_2n_3, when n_2, n_3 run over a pair of indices B, B^* (or D, D^* etc.), since the corresponding wave functions are very similar. Therefore, the kernel $K_n(E)$ in (18) also does not depend on indices n_2n_3 and can be written as

$$K_n(E) = \int \frac{d^3\mathbf{k}}{(2\pi)^3} \frac{e^{-(\mathbf{k}^2/2\beta_2^2)}}{2\omega_\pi(\mathbf{k})(E_n(\mathbf{k}) + \omega_\pi(\mathbf{k}) - E)}. \quad (34)$$

Defining as in (14)

$$\zeta_{nn'}(E) = \frac{1}{N_c} \sum_{n_2 n_3} \int \frac{d^3\mathbf{p}}{(2\pi)^3} \frac{\chi_{nn_2n_3}(\mathbf{p})\chi_{n'n_2n_3}(\mathbf{p})}{E_{n_2}(\mathbf{p}) + E_{n_3}(\mathbf{p}) - E}, \quad (35)$$

one has a system of equations (17), from which one defines resonance energy [17]

$$\det[1 - \hat{K}(E)\hat{\zeta}(E)] = 0, \quad (36)$$

where $(\hat{K})_{nn'} = K_n\delta_{nn'}$ and $(\hat{\zeta})_{nn'} = \zeta_{nn'}$.

Note that $\chi_{nn_2n_3}$ depends on polarization states of all particles, and that of n (index i in (29) and (30)) can be fixed, while one should sum up in (35) over spin and isospin projection of particles n_2, n_3.

At the end of this section we consider the contribution of pion-quarkonium resonance into production cross sections of the final state $(Q\bar{Q})_{n'}\pi\pi$. In the zeroth approximation, the amplitude for the transition $(Q\bar{Q})_n \to (Q\bar{Q})_{n'}\pi\pi$ was calculated in [24–26].

$$w_{nm}^{(\pi\pi)}(E) = \sum_{n_2n_3} \frac{d^3p}{(2\pi)^3} \frac{J^{(1)}_{nn_2n_3}(\mathbf{p},\mathbf{k}_1)J^{*(1)}_{mn_2n_3}(\mathbf{p},\mathbf{k}_2)}{E - E_{n_2n_3}(\mathbf{p}) - \omega_\pi(\mathbf{k}_1)} + (1 \leftrightarrow 2)$$
$$- \sum_{n_2'n_3'} \frac{d^3p}{(2\pi)^3} \frac{J^{(2)}_{nn_2'n_3'}(\mathbf{p},\mathbf{k}_1,\mathbf{k}_2)J^{*}_{mn_2'n_3'}(\mathbf{p})}{E - E_{n_2'n_3'}(\mathbf{p}) - (\omega_\pi(\mathbf{k}_1) + \omega_\pi(\mathbf{k}_2))}$$
$$- \sum_{n_2''n_3''} \frac{d^3p}{(2\pi)^3} \frac{J_{nn_2''n_3''}(\mathbf{p})J^{*(2)}_{mn_2''n_3''}(\mathbf{p},\mathbf{k}_1,\mathbf{k}_2)}{E - E_{n_2''n_3''}(\mathbf{p})} \quad (37)$$

Here, $J^{(1)}_{nn_2n_3} \equiv J^{(\pi)}_{nn_2n_3}(\mathbf{p},\mathbf{k})$ and

$$J^{(2)}_{nn_2n_3}(\mathbf{p},\mathbf{k}_1,\mathbf{k}_2) \equiv \frac{1}{\sqrt{N_c}} \bar{y}^{(\pi\pi)}_{123} e^{-((\mathbf{k}_1+\mathbf{k}_2)^2/4\beta_2^2)} e^{-((c\mathbf{p})^2/\Delta_n)} \times I_{nn_2n_3}(c\mathbf{p}); \quad (38)$$

with

$$\bar{y}^{(\pi\pi)}_{123} = \frac{M_\omega \boldsymbol{\pi\pi} 21}{f_\pi^2} \frac{\bar{y}_{123}}{\sqrt{2\omega_\pi(\mathbf{k}_1)2\omega_\pi(\mathbf{k}_2)V_3^2}}, \quad (39)$$

while $J_{nn_2n_3}(\mathbf{p})$ is the pionless overlap integral (2), where $\mathbf{k} \equiv 0$, and $\bar{y}^{(h)}_{123} \to \bar{y}_{123} = M_\omega \frac{i}{\omega_q}(q_i - \frac{p_i\omega_q}{2(\omega_q+\omega_Q)})$.

Looking at (37), one can realize that it can be written as

$$w_{nm}^{(\pi\pi)}(E) = {}^{(1)}w_{nm}^{(\pi\pi)}(E) - {}^{(2)}w_{nm}^{(\pi\pi)}(E) \quad (40)$$

and the first two terms of ${}^{(1)}w_{nm}^{(\pi\pi)}(E)$ are

$${}^{(1)}w_{nm}^{(\pi\pi)} = \varphi(\mathbf{k}_1)\zeta_{nm}(E')\varphi(\mathbf{k}_2) + \varphi(\mathbf{k}_2)\zeta_{nm}(E'')\varphi(\mathbf{k}_1), \quad (41)$$

where ζ_{nm} depends on the energy E' and E'' of the $(Q\bar{Q})\pi_2$ and $(Q\bar{Q})\pi_1$ systems, respectively; for its Lorenz invariant definition, see below. It is clear that these terms are the first terms of the whole rescattering series, depicted in Fig. 3, which can be summed up as follows:

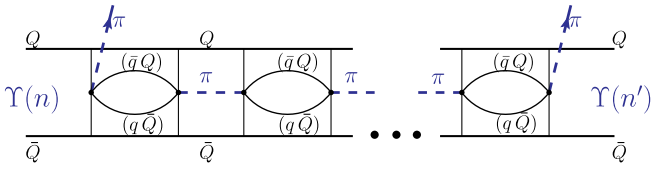

FIG. 3 (color online). Rescattering series yielding a possible pole structure in $(\Upsilon(n')\pi)$. (Contribution to a_{nm}.)

$${}^{(1)}w_{nm}^{(\pi\pi)} \to {}^{(1)}W_{nm} = \varphi(\mathbf{k}_1)\left(\zeta \frac{1}{1 - K\zeta}\right)_{nm} \varphi(\mathbf{k}_2) + \varphi(\mathbf{k}_2)\left(\zeta \frac{1}{1 - K\zeta}\right)_{nm} \varphi(\mathbf{k}_1). \quad (42)$$

Note that for the transition $\Upsilon(n) \to \Upsilon(n')\pi\pi$, $\zeta(E')$ and $K(E')$ in the first term in (42) depend on the invariant mass $M^{(1)}_{\text{inv}}$ of $\Upsilon(n')\pi_2$, while in the last term on the rhs of (42), $\zeta(E'')$ and $K(E'')$ depend on the invariant mass $M^{(2)}_{\text{inv}}$ of $\Upsilon(n')\pi_1$,

$$M^{(i)}_{\text{inv}} = \sqrt{M_n^2 - 2M_n\omega_i + m_\pi^2}, \qquad i = 1, 2.$$

We now turn to the last two terms in (37), which contain a two-pion vertex, shown in Fig. 4, and take into account that the dependence on $\mathbf{k}_1$, $\mathbf{k}_2$ there is contained in the factor $\varphi(\mathbf{k}_1 + \mathbf{k}_2)$, as was shown in [24,25], as well as in the series shown in Fig. 5 (and the similar one with $\mathbf{k}_1 \leftrightarrow \mathbf{k}_2$). Hence, the total amplitude of (n, m) transition with emission of two pions can be written as

$$w_{nm}^{(\pi\pi)} \equiv \mathcal{M}_{nm} = \varphi(\mathbf{k}_1)\varphi(\mathbf{k}_2)a_{nm} - \varphi(\mathbf{k}_1 + \mathbf{k}_2)b_{nm} \quad (43)$$

where

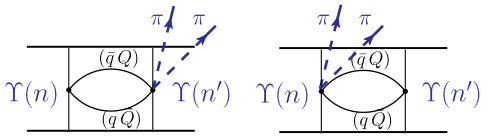

FIG. 4 (color online). First order (in ζ) contributions to the factor b_{nm} in Eq. (43).

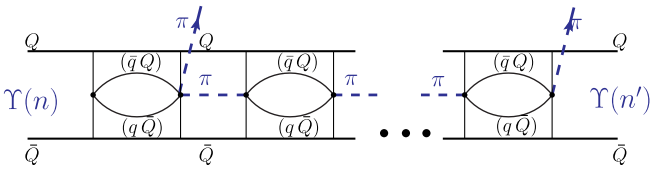

FIG. 5 (color online). Rescattering series including double pion production vertex. (Contributing to b_{nm}.)

$$a_{nm} = \left(\zeta(E')\frac{1}{1-K(E')\zeta(E')}\right)_{nm} + (E' \to E'')_{nm}$$
$$b_{nm} = \left(\zeta(E')\left(\frac{1}{1-K(E')\zeta(E')} + (E' \to E'')\right)\right)_{nm}. \quad (44)$$

One can see that (43) satisfies the Adler condition

$$a_{nm}(k_i = 0) = b_{nm}(k_i = 0), \qquad \mathcal{M}_{nm}(\mathbf{k}_1 = 0) = 0, \quad (45)$$

and for not very large $\mathbf{k}_1$, $\mathbf{k}_2$ one can write approximately

$$\mathcal{M}_{nm} \approx a_{nm}(\varphi(\mathbf{k}_1)\varphi(\mathbf{k}_2) - \varphi(\mathbf{k}_1 + \mathbf{k}_2)). \quad (46)$$

The probability of transition $(Q\bar{Q})_n \to (Q\bar{Q})_{n'}\pi\pi$ is

$$dw((n) \to (n')\pi\pi) = |\mathcal{M}_{nn'}|^2 \frac{d^3\mathbf{k}_1}{(2\pi)^3}\frac{d^3\mathbf{k}_2}{(2\pi)^3}\frac{\pi}{2\omega_1\omega_2} \times \delta(E_{n'} + \omega_\pi(\mathbf{k}_1) + \omega_\pi(\mathbf{k}_2) - E_n) \quad (47)$$

and the di-pion decay width is

$$\Gamma^{(\pi\pi)}_{nn'} = \int dw((n) \to (n')\pi\pi) = \int d\Phi |\mathcal{M}_{nn'}|^2 \quad (48)$$

where $d\Phi$ is the phase space factor

$$d\Phi = \frac{1}{32\pi^3}\frac{(M_n^2 + M_{n'}^2 - q^2)(M_n + M_{n'})}{4M_n^3} \times \sqrt{(\Delta M)^2 - q^2}\sqrt{q^2 - 4m_\pi^2}\, dq\, d\cos\theta \quad (49)$$

with the notations

$$\Delta M = M_n - M_{n'}$$
$$q^2 \equiv M^2_{\pi\pi} = (k_1 + k_2)^2 = (\omega_1 + \omega_2)^2 - (\mathbf{k}_1 + \mathbf{k}_2)^2. \quad (50)$$

Finally, one can also study the process $e^+e^- \to (Q\bar{Q})_{n'}\pi\pi$, with the amplitude

$$A_{n'}(E) = \sum_{m,n} c_m \left(\frac{1}{\hat{E} + \hat{w} - E}\right)_{mn} \mathcal{M}_{nn'} \quad (51)$$

where $\mathcal{M}_{nn'}$ is given in (43) and $c_m = \frac{4\pi\alpha e_Q\sqrt{6}}{E^2}\Psi^{(m)}_{Q\bar{Q}}(0)$ so that the contribution ΔR of $(Q\bar{Q})_{n'}\pi\pi$ to the hadronic ratio R is

$$\Delta R((n')\pi\pi) = \frac{72\pi e_Q^2}{E^2}\left|\sum_{n,m}\Psi^{(n)}_{Q\bar{Q}}(0) \times \left(\frac{1}{\hat{E} + \hat{w} - E}\right)_{nm}\mathcal{M}_{mn'}\right|^2 d\Phi. \quad (52)$$

We now turn to an example of possible pionic bottomonium state in the reaction $\Upsilon(5S) \to (\Upsilon(n')\pi)\pi$, which can proceed through the chains

TABLE I. List of thresholds (in GeV).

Threshold	$E_{\rm th}$	Threshold	$E_{\rm th}$
BB^*	10.605	$\Upsilon(1S)\pi$	9.60
B^*B^*	10.650	$\Upsilon(2S)\pi$	10.16
$B_sB_s^*$	10.780	$\Upsilon(3S)\pi$	10.495
$B_s^*B_s^*$	10.830	$\Upsilon(4S)\pi$	10.720
		$\Upsilon(5S)\pi$	11.00

$$\Upsilon(5S) \to \sum_{n_2n_3}(B\bar{B})_{n_2n_3}\pi \to \sum_{n'}(\Upsilon(n')\pi)\pi. \quad (53)$$

We are interested in possible poles in the $J^P = 1^+$ channel of connected $(B\bar{B})_{n_2n_3}$ and $\Upsilon(n')\pi$ states, which are given by the equation

$$\det[\delta_{nn'} - K_n(E)\zeta_{nn'}(E)] = 0. \quad (54)$$

Neglecting first nondiagonal elements of $\zeta_{nn'}$, one has an equation for E

$$K_n(E)\zeta_{nn}(E) = \frac{1}{N_c}\sum_{n_2n_3}\int\frac{d^3\mathbf{p}}{(2\pi)^3}\frac{\chi^2_{nn_2n_3}(\mathbf{p})}{E_{n_2}(\mathbf{p}) + E_{n_3}(\mathbf{p}) - E} \times \int\frac{d^3\mathbf{k}}{(2\pi)^3}\frac{\varphi^2(\mathbf{k})}{2\omega_\pi(k)(E_n(\mathbf{k}) + \omega_\pi(\mathbf{k}) - E)} = 1. \quad (55)$$

One can easily recognize in (55) the norm of the kernel of the integral equation (8).

The analysis of (55) starts with the list of thresholds in $(B\bar{B})_{n_2n_3}$ and in $\Upsilon(n')\pi$ channels in Table I. One can see that the most important combination is $\Upsilon(3S)\pi \leftrightarrow BB^*$, B^*B^* with the additional contribution of $\Upsilon(2S)\pi$, $\Upsilon(1S)\pi$ and $B_sB_s^*$, $B_s^*B_s^*$ as a next step. Since the maximal energy of our systems in the reaction (53) is $M(5S) - m_\pi = 10.725$ GeV, one is mostly interested in the energy region 9.78 GeV $\le E \le$ 10.72 GeV.

V. RESULTS FOR $\Upsilon(5S) \to \Upsilon(n'S)\pi\pi$

In this section, we study numerical results for the reaction $\Upsilon(5S) \to \Upsilon(n'S)\pi\pi$, and we shall be interested mainly in the possible appearance of resonance-like structures in the systems $\Upsilon(n'S)\pi$, $n' = 1, 2, 3$. The resulting equations for differential and total probabilities are given in Eqs. (44) and (46)–(48). The coefficients $\bar{y}^{(\pi)}_{123}$ and parameters of $\Upsilon(nS)$ and B, B^* wave functions, needed for the calculation of ζ_{nm}, are given in Eqs. (29) and (30) and Appendices A and B.

It was assumed above that the knowledge of wave functions and channel coupling constant M_ω (one for all types of strong decays) can describe all CC phenomena and, in particular, level shifts due to the CC. However, at this point one encounters the fundamental difficulty which was studied in [34] and is not still resolved. The point is that, assuming a constant CC not depending on participants

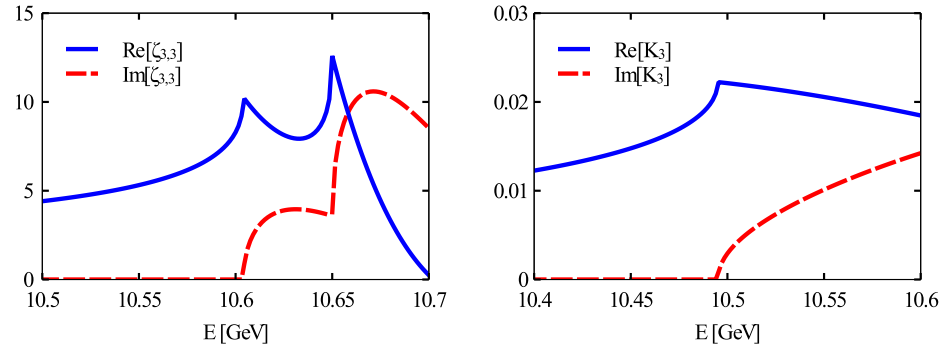

FIG. 6 (color online). Real (solid line) and imaginary (dashed line) parts of $\zeta_{33}(E)$ and $K_3(E)$ [see Eqs. (34) and (35)]. One can see cusp structures at the thresholds BB^*, B^*B^* and $\Upsilon(3S)\pi$, correspondingly.

of the decay process, one obtains huge shifts of energy levels (several hundreds of MeV) due to mixing with higher states. (To improve the situation, in [18] a cut-off coefficient $\kappa \approx 0.5$ was introduced for contribution of higher levels.) This calls for a detailed scrutiny of our matrix elements $J^{(h)}_{nn_2n_3}(\mathbf{p}, \mathbf{k})$ and basic matrix elements (without hadron emission) $J_{nn_2n_3}(\mathbf{p})$, entering in the expressions for energy shifts, see [17] for details. Indeed, in Eq. (2) one can see that the string in the original hadron n, placed between points $\mathbf{u}$, $\mathbf{v}$ is decaying at point $\mathbf{x}$ into two hadrons, placed between $\mathbf{u}$, $\mathbf{x}$, and $\mathbf{x}$, $\mathbf{v}$, respectively. It is clear that when the point $\mathbf{x}$ is far away from the center of the string $\mathbf{u}$, $\mathbf{v}$, the string-breaking process does not occur. Replacing distances between points by typical radii R_n, R_{n_2}, R_{n_3} of states n, n_2, n_3, one obtains the condition (for $R_{n_2} \approx R_{n_3}$) $R^2_{n_2} \lesssim \frac{1}{4}R^2_n + \rho^2$ where ρ is the typical string width, $\rho \approx 2\lambda \approx 0.3$ fm [35,36]. The corresponding factor can be rigorously deduced in the formalism of [28], and the resulting cutoff strongly decreases the CC between states with incomparable sizes. This is taken into account below by assuming different M_ω for different decay channels. We take for M_ω the value 1.0 GeV in case of $n = 4, 5$. For $n = 1, 2, 3$ we take $M_\omega = 0.1$, 0.2 and 0.3 GeV, respectively, to take into account decay mismatch between the sizes of $\Upsilon(nS)$ and $B\bar{B}^*$ systems, since $R(1S) = 0.2$ fm and $R(2S) = 0.4$ fm, while $R(B) \approx R(B^*) \approx 0.5$ fm. This mismatch is not taken into account for simplicity reasons in the general definition of the overlap integral (2).

In the beginning, we have estimated $K_n(E)$ and $\zeta_{nm}(E)$ in (55) for $n, m = 1, 2, 3, 4, 5$ using parameters of SHO functions, which were used before in [25,26]; they are given in the Appendix B. Real and imaginary parts of $\zeta_{33}(E)$ and $K_3(E)$ are given in Fig. 6. The possibility of peaks, e.g. in the $\Upsilon(n'S)\pi$ system, is demonstrated in Fig. 7, where we plot the quantity $|a_{5n'}|^2$ for $n' = 1, 2, 3$, respectively (or more exactly the first term of (44)) as function of the invariant mass $M^{(1)}_{\text{inv}}$. One can see sharp peaks near the thresholds BB^*, B^*B^* at 10.6 and 10.65 GeV, respectively. In the total distributions, however, a more complicated combination of terms enters, as seen from (44), and one should calculate a symmetrized in $M^{(1)}_{\text{inv}}, M^{(2)}_{\text{inv}}$ expression, and moreover take into account appropriate phase space factor. One can associate these peaks with poles, situated in the vicinity of these thresholds (see discussion in Appendix C).

Note that two peaks in Fig. 7 occur from combination $\Upsilon(n'S)\pi_1$. However, in the full decay distribution $dw((5) \to (n')\pi\pi)$ the symmetrized sum (44) enters, which produces an additional mirror reflected pair of peaks in dw if considered as function of $M^{(1)}_{\text{inv}}$, q since

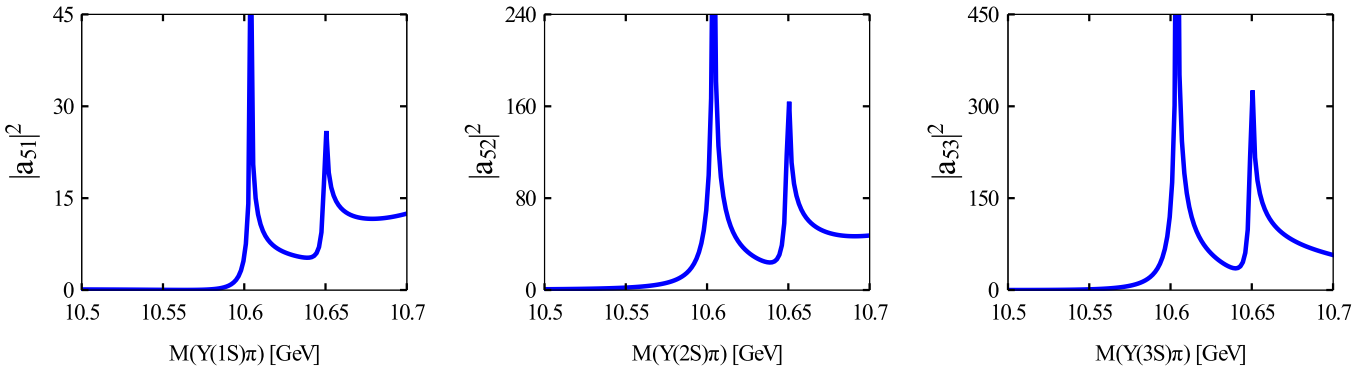

FIG. 7 (color online). Modulus squared of the first term in (44) $|a_{nn'}|^2$ as a function of the invariant mass of $(\Upsilon(n'S)\pi)$, computed for the reaction $\Upsilon(5S) \to \Upsilon(n'S)\pi\pi$, $n' = 1, 2, 3$.

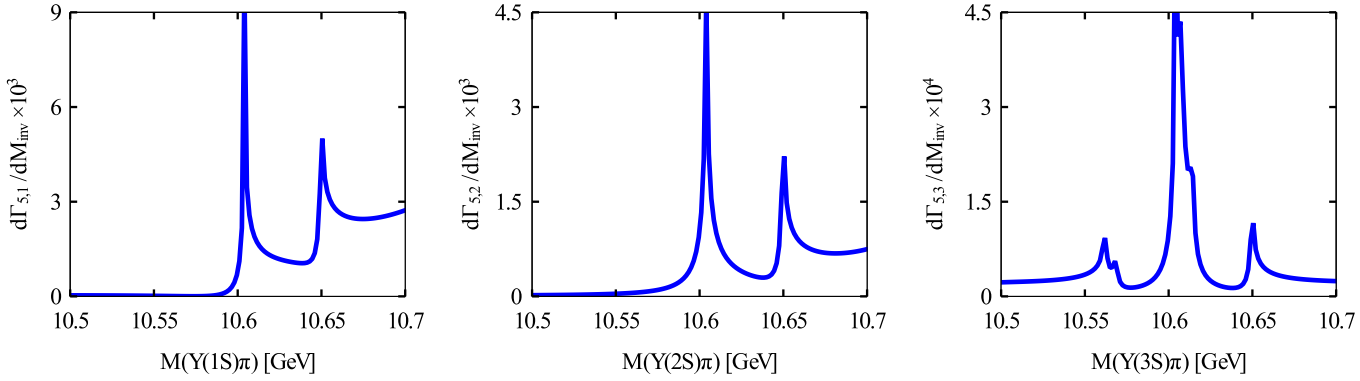

FIG. 8 (color online). The distribution $d\Gamma_{nn'}/dM_{inv}$ for the transition $\Upsilon(nS) \to \Upsilon(n'S)\pi\pi$ as a function of the invariant mass of $(\Upsilon(n'S)\pi)$ for $n' = 1, 2, 3$.

$$(M^{(1)}_{\rm inv})^2 + (M^{(2)}_{\rm inv})^2 = M^2_n + M^2_{n'} + 2m^2_\pi - q^2. \qquad (56)$$

The full probability distribution (47) contains the symmetric sum of two rescattering series for $\Upsilon(n'S)\pi_1$ and $\Upsilon(n'S)\pi_2$, respectively. When plotted as a function of $M^{(1)}_{\rm inv}$, it contains both poles of the first series at $M^{(1)}_{\rm inv} = 10.610$ and 10.650 GeV, and also poles from the second series at the points $M^{(1)}_{\rm inv}(M^{(2)}_{\rm inv} = 10.610,\ 10.650)$ defined by Eq. (56). In this way one obtains Fig. 8, where for the case $(n, n') = (5, 1)$ and $(5, 2)$ the secondary poles are out of mass interval, while for the case of $(5, 3)$ the pair of secondary poles overlap with the proper poles of $M^{(1)}_{\rm inv}$. In an experiment, one can separate points on Dalitz plot relating to $M^{(1)}_{\rm inv}$ and $M^{(2)}_{\rm inv}$, which results in two plots with the same pair of peaks.

Recently, experimental data on the reaction $\Upsilon(5S) \to \Upsilon(n'S)\pi\pi$, $n' = 1, 2, 3$ appeared in [37], and the experimental distributions $dw((5) \to (n')\pi\pi)$ are presented in Fig. 5 of [37] as functions of $\min\{M^{(1)}_{\rm inv}, M^{(2)}_{\rm inv}\}$ and $\max\{M^{(1)}_{\rm inv}, M^{(2)}_{\rm inv}\}$. In order to compare our results with experimental data, we calculate distribution (47) in terms of invariant masses of $\Upsilon(n'S)\pi$ and $\pi\pi$ systems. We use expressions (46) and (49) and formulas from [24] to express quantities like $\omega_\pi(\mathbf{k}_1)$, $(\mathbf{k}_1 + \mathbf{k}_2)^2$, etc. via variables $(q, M_{\rm inv})$. After integration over q, we obtain the distribution in terms of $M_{\rm inv}(\Upsilon(n'S)\pi)$. The result is presented on Fig. 8. Comparing experimental data (left and right plots, glued together for $n' = 3$ and left plots for $n' = 1, 2$ on Fig. 5 from [37]) with our theoretical calculations, one can see a close similarity in the general form and position of $Z_b(10610)$ and $Z_b(10650)$ peaks, which in both cases appear at BB^*, B^*B^* thresholds for all available $n' = 1$, 2, 3. We do not intend to reproduce here all features of experimental data, which depend strongly on details of wave function profile, but we study mostly the dynamics of process. For the better description, we only slightly changed w.f. of $\Upsilon(nS)$, calculated in single-channel approximation in Appendix B, $\beta_{\rm new} = \beta + 0.2$. This effect could appear due to mixing of a given state $\Upsilon(nS)$ with $\Upsilon(n'S)$ and $\Upsilon(n''D)$, which is not accounted for in our rescattering series of Fig. 3. A more detailed quantitative comparison of our data with experiment [37], and decay distributions as functions of $q \equiv M_{\pi\pi}$ and $\cos\theta$ are now in progress and will be reported elsewhere.

VI. CONCLUSIONS AND OUTLOOK

Summarizing our results, we shall stress the main features of our approach. We have considered the interaction of a light hadron with heavy quarkonium, arising solely due to transition to intermediate states of two heavy-light mesons. No direct interaction between light hadron and heavy quarkonium or else between two heavy-light mesons is assumed, therefore our dynamics has nothing to do with molecular states in the strict sense. Our mechanism is also distinct from dynamics of $(4q)$ or hybrid states.

At this point, it is important to discuss the suggested mechanism in more general terms. We have exploited the Lagrangian, which was derived earlier by one of the authors, see [24] and references therein, and recently given an explicit form of string breaking plus meson emission Lagrangian in Ref. [28]. It is important that this Lagrangian does not contain any extra parameters in addition to string tension σ and f_π in case of pions, and the resulting amplitude for $\pi\pi$ emission satisfies the Adler condition, as shown in [24]. Having this fundamental instrument, it is tempting to use it in realistic situation, which was done in [24–28] for bottomonium transitions and this application was for the most part successful, namely, angular and mass di-pion distributions do generally agree with the experiment for all transitions of $\Upsilon(n, n')\pi\pi$, $n = 2$–5, $n' = 1, 2, 3$ and as well as production of BB, BB^*, B_sB_s etc. There are few disagreements, e.g. in absolute value of $(2, 1)$ transition, angular dependence for $(5, 1)$. With all this, one should consider other possible mechanisms, and the limitations of the

exploited formalism. First of all, for small size bottomonium, like $\Upsilon(1S)(r = 0.2$ fm) or $J/\psi(r = 0.4$ fm) the string-breaking process with string radius of 0.3 fm and the size of hadron of 0.6 fm, should be highly nonlocal and therefore formalism is subject to strong corrections. This point is discussed at the beginning of Sec. V, where it was argued, that for the (5, 1) transition the numerical value of the string-breaking parameter M_ω (playing the role of σ) should be strongly reduced. We see this effect as the result of small overlap of $\Upsilon(1S)$ and BB^*, when real size of the string is taken into account, but we cannot exclude that another type of configuration, like that discussed in Ref. [9], plays a role here. For the decays of $\Upsilon(5S)$ or $\Upsilon(4S)$ into BB^*, $BB^*\pi$, the situation is different—the corresponding sizes are $r_5 = 1.1$ fm, $r_4 = 0.9$ fm, $r_3 = 0.7$ fm, while $r_B \approx r_{B^*} = 0.5$ fm. Therefore, the string-breaking Lagrangian with pions used in the paper is valid (and even more valid for charmonia, where sizes of states are higher) at least for higher bottomonia states. An additional tension between sizes of the decaying state and its product may be created by the emission at the string-breaking point of one or two mesons, as it happens in the pionic string-breaking vertices in Eq. (2), where the meson is emitted at the point x and its size is not taken into account. However, this is a direct consequence of the chiral theory formalism, and in the paper of one of the author, in [38], and later in [28], it was shown that the resulting Lagrangian has the structure of Eq. (28) of [28] and in the local limit coincides with the Weinberg Lagrangian. The nonlocality of this Lagrangian is of the order of $\lambda = 0.2$ fm, while chiral theory assumes always the local limit. Therefore, mesons are assumed to be produced as local objects, with the corresponding Z factors introduced in [28] to account for perturbative and nonperturbative renormalization. Hence, in the transition from the nonlocal form to the local form, like that in our Eq. (3), one neglects the nonlocality in the same way as it is done in the derivation of chiral Lagrangian in the cited above paper, but in our case it is only the limit of λ tending to zero, while for the total chiral Lagrangian the nonlocality is more complicated. We have not attempted here the calculation of Z factors of pions since they enter in the product with the factor M_ω, which is also renormalized due to finite string length and radius, as discussed in text above, and therefore one can consider the overall renormalization of the product.

Another point is whether this mechanism is dominant. A possible competing mechanism is the string decay of the initial $\Upsilon(nS)$ state into a pair of higher B mesons, which subsequently decay into pions and B, B^*, e.g. into $B_1(5721)$ or $B_2(5747)$. However, the pionic widths of those are small and overlap matrix elements with $\Upsilon(nS)$ are suppressed due to p-wave structure of these mesons. Therefore, we do not see other competing mechanisms in our type of approach, but effectively the string-breaking process can be highly nonlocal for lowest $\Upsilon(nS)$ states. Another picture of hadro-quarkonia can be based on a molecular-type mechanism, similar to one suggested in Ref. [9]. In our opinion, there is no contradiction, and we have worked out the generalized mechanism where in addition to the basic vertices described in the paper the BB^*, B^*B^* (or else $\Upsilon\pi$) interaction is also taken into account. The resulting equations are the same as in (42) of the paper, but with a more general form of $\zeta_{nm}(E)$, depending on scattering lengths of BB^*, B^*B^*. This work is now in progress and should answer the question how hadron-hadron interaction modifies results of strong channel coupling.

We have explicitly exploited the transition vertex which was constructed from the fist principles, for the strong decay with emission of a light hadron. As a result, all dynamics are defined by the overlap integrals of all wave functions involved, i.e. heavy quarkonia and heavy-light mesons. The latter have been found in [39] from the relativistic Hamiltonian, containing minimal input: pole (current) quark masses, string tension and saturated α_s (to two loops). Results of our work given in Figs. 7 and 8, for the case of pion-bottomonium system agree with the recent experimental data [37], at least qualitatively. More detailed calculations are still needed to check all results quantitatively vs experiment, and this program is now under study. Other systems should be treated as well, e.g. πh_b studied in [37], and the series of $Z(4430)$, $Z_1(4050)$, $Z_2(4250)$ resonances in the $(c\bar{c})\pi$ system. All formalism used above for bottomonium can be applied to the charmonium case without modifications; for the axial vector charmonium or bottomonium (h_b, χ_b, h_c, χ_c) one can use transition vertices, given in Appendices A and B, and symmetry properties of the whole amplitude will be different. This work is now in progress.

One should stress at this point that resonances found above in the $\Upsilon(n'S)\pi$ system are specifically multichannel ones, in the sense that they belong (and appear) in all n' channels and are given by zeros of $\det[1 - \hat{K}\hat{\zeta}]$.

At this point, it is convenient to compare predictions of molecular and CC models for the positions of resonances. As one can see in Fig. 7, our CC model predicts sharp peaks at $\bar{B}B^*$, $\bar{B}^*B^*$ thresholds (possibly due to virtual multichannel poles) in all $\Upsilon(n'S)\pi$ ($n' = 1, 2, 3$) channels, and this effect is due to combined contribution of $\hat{\zeta}$ and $\hat{K}$ terms, i.e. pure CC effect. In contrast to that, the pure molecular picture, when poles in the BB^*, B^*B^* systems appear due to direct internal interaction (i.e. without $\pi\Upsilon(nS)$ channels), the poles appear in all $\zeta_{nn}(E)$ terms near corresponding thresholds. This can be seen simply in the definition of $\hat{\zeta}(E)$ in (35), where $\chi_n\chi_{n'}$ is multiplied by the free $BB^*(B^*B^*)$ Green's function. In case of strong interaction in BB^*, B^*B^* systems, this Green function is replaced by the exact one and should contain pure molecular poles i.e. $\zeta_{nm}(E) = \frac{C_nC_m}{E_0 - E}$. Insertion of this form into the $\det[1 - \hat{K}\hat{\zeta}] = 0$ yields the n-th order equation for roots in

energy, and these n roots are all strongly displaced from the original places at the thresholds for large $K\zeta$ coupling (large C_n), and are almost degenerate n poles at thresholds for small coupling. Both pictures are different from the experimental data—the same two poles at $\bar{B}B^*$ and $\bar{B}^*B^*$ in all $\pi\Upsilon(nS)$ and $\pi h_b(mP)$ channels. Thus the situation with the only pole at each threshold is possible and characteristic for our multichannel CC resonance and is unlikely for pure molecular states.

Another property is that resonances appear most likely when thresholds in $\hat{K}_n$ and $\hat{\zeta}_{nn}$ for some n are close to each other, and then this channel n will be the dominant one, making $\det[1 - \hat{K}\hat{\zeta}]$ close to zero. In the case of $\pi\Upsilon(n'S)$, the dominant channels are those with $n' = 3, 4$, as can be seen from Table I in Sec. IV. Therefore, the visible channel $h(Q\bar{Q})_{n'}$, where a peak is found, is not necessarily the dominant one as might be in the case of $Z(4430)$ with a peak seen in $\pi^+\psi'$ channel. The dynamical reason, why proximity of thresholds is favorable for the appearance of a resonance, is that both $\mathrm{Re}[K_n(E)]$ and $\mathrm{Re}[\zeta_{nn}(E)]$ are decreasing fast enough away from thresholds, making their product maximal for the coinciding thresholds.

In all discussions above, the notion of resonances (or virtual and real poles) was stressed, and hence the whole sum of rescattering series as in Figs. 3 and 5, were considered. But it is possible, that already the first terms of this series can contribute to enhanced correlations, which look like bumps in decay distributions. This approach was considered in two recent papers [40,41], and is especially important in the case, when high spins and angular momenta are involved. Relation of this approach to our methods in the present paper seems to be practically important and the corresponding work is planned for the future.

Recently, several papers appeared [42,43] where $Z_b(10610)$ and $Z_b(10650)$ are considered as molecular states and treated in the QCD sum rule method [42], while in [43] these states were originally supported to be χ_{b_1} and χ'_{b_1} shifted to the BB^* and B^*B^* thresholds (as it happens in $X(3872)$ case). As was argued above in both cases, the poles produced appear in $\zeta_{nn'}$ and would be strongly shifted in the rescattering series of Fig. 1, yielding five peaks at different masses in $\Upsilon(nS)\pi$, $h_b(mP)\pi$, $n = 1, 2, 3$ $m = 1, 2$. In [44], an interesting analysis of $\Upsilon(5S) \to \Upsilon(2S)\pi\pi$ decay is presented, demonstrating important contribution of $Z_b(10610)$, $Z_b(10650)$ to the decay distribution in $M(\pi^+\pi^-)$ and $\cos\theta$ a detailed comparison of these results with our approach and previous results in [26] is now in progress.

ACKNOWLEDGMENTS

The authors are grateful to A. M. Badalian, R. Mizuk and P. N. Pakhlov for many useful discussions. The financial support of Dynasty Foundation to V. D. O. and RFBR Grant No. 09-02-00 620a is gratefully acknowledged.

APPENDIX A: CALCULATION OF THE TRANSITION KERNEL $\bar{y}^{(h)}_{123}$

We use here, as well as in [17,24,25], the spin-tensor representation of wave functions and Z factors instead of technic of Clebsch-Gordan coefficients. We start with the (4×4) fully relativistic technic given in [24,25], where $\bar{y}_{123}$ can be written through the so-called Z factors (we omit the superscript h for time being, cf. Eq. (A2.24) of [24])

$$\bar{y}_{123} = \frac{Z_{123x}}{\sqrt{\Pi_{i=1,2,3} Z_i}}, \tag{A1}$$

where Z_{123x} and Z_i are Z factors for the total process and for individual hadrons, respectively, participating in the transition process $1 \to 23$ or $1 \to 23h$, shown in Fig. 9. Defining projection factors for quarks and antiquarks $\Lambda^{\pm}_k$, where subscript k refers to light quarks, $k = q$, or heavy quarks, $k = Q$, one can write

$$Z_{123x} = \mathrm{tr}(\Gamma_1\Lambda^+_Q\Gamma_2\Lambda^-_q\Gamma_x\Lambda^+_q\Gamma_3\Lambda^-_Q), \tag{A2}$$

$$Z_i = \mathrm{tr}(\Gamma_i\Lambda^+_k\Gamma_i\Lambda^-_k), \tag{A3}$$

and

$$\Lambda^{\pm}_k = \frac{m_k \pm \omega_k\gamma_4 \mp i p^{(k)}_i\gamma_i}{2\omega_k}, \qquad k = q, Q. \tag{A4}$$

Note, that the sum over (i) in (A4) is for $i = 1, 2, 3$, also in the c.m. system $p^{(1)}_i = -p^{(2)}_i \equiv p_i$, while m_k is the current quark mass and ω_k is the average kinetic energy of quark k in the hadron.

The operators Γ_i correspond to quantum numbers of a hadron, and are given in Table II below, while Γ_x refers to the process under investigation, for the case when no hadron is emitted, $\Gamma_x = 1$, while for the pion emission $\Gamma^{(\pi)}_x = \gamma_5$ and for vector particles $\Gamma^{(v)}_x = \gamma_i$.

In this way, one obtains

$$Z_{D,B} = \frac{\Omega - \omega}{\Omega}, \qquad Z_{\psi,\Upsilon} = \frac{\frac{4}{3}\Omega^2_{\psi,\Upsilon} + \frac{2}{3}m^2_{c,b}}{\Omega^2_{\psi,\Upsilon}}, \tag{A5}$$

where $\Omega_{D,B} = \langle\sqrt{\mathbf{p}^2 + m^2_{c,b}}\rangle_{D,B}$, $\Omega_{\psi,\Upsilon} = \langle\sqrt{\mathbf{p}^2 + m^2_{c,b}}\rangle_{\psi,\Upsilon}$ are calculated in [24] and given in Appendix A of [14].

Examples of relativistic (4×4) expressions of $\bar{y}_{123}$ are given in [24,25], e.g. for $(1^{--})_n \to BB^*\pi(DD^*\pi)$ and $(1^{--})_n \to B^*B^*\pi(D^*D^*\pi)$, $\bar{y}^{(\pi)}_{123}$ are given in (29) and (30), while for $(1^{--}) \to BB^*$

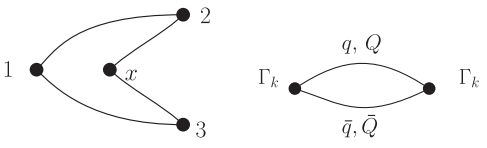

FIG. 9. Decay matrix vertices.

TABLE II. Bilinear operators $\bar{\psi}\Gamma_i\psi$ and their (2×2) forms. We used the following notations $\psi=(v,w)^t$, $\rho_{ik}\equiv\sigma_i\overleftrightarrow{\partial}_k+\sigma_k\overleftrightarrow{\partial}_i-\frac{2}{3}\sigma_l\overleftrightarrow{\partial}_l\delta_{ik}$; $\omega_{ik}\equiv\overleftrightarrow{\partial}_i\overleftrightarrow{\partial}_k-\frac{1}{3}\delta_{ik}(\overleftrightarrow{\partial})^2$, and $\hat{\partial}\equiv\overleftrightarrow{\partial}_i\gamma_i$. See details in Appendix B of [17].

J^{PC}	$^{2S+1}L_J$	Γ_i	(2×2) form	$\Gamma_{\rm red}$
0^{-+}	$^1S_0$	$-i\gamma_5$	$\tilde{v}^c v-\tilde{w}^c w$	$\frac{1}{\sqrt{2}}$
1^{--}	$^3S_1$	γ_i	$-(\tilde{v}^c\sigma_i v+\tilde{w}^c\sigma_i w)$	$\frac{1}{\sqrt{2}}\sigma_i$
1^{+-}	$^1P_1$	$-i\gamma_5\overleftrightarrow{\partial}_i$	$\tilde{v}^c\overleftrightarrow{\partial}_i v-\tilde{w}^c\overleftrightarrow{\partial}_i w$	$\sqrt{\frac{3}{2}}n_i$
0^{++}	$^3P_0$	1	$i(\tilde{v}^c w-\tilde{w}^c v)$	$\frac{1}{\sqrt{2}}\boldsymbol{\sigma}\mathbf{n}$
1^{++}	$^3P_1$	$\gamma_i\gamma_5$	$-(\tilde{v}^c\sigma_i w+\tilde{w}^c\sigma_i v)$	$\frac{\sqrt{3}}{2}e_{ikl}\sigma_k n_l$
2^{++}	$^3P_2$	$\gamma_i\overleftrightarrow{\partial}_k+\gamma_k\partial_i-\frac{2}{3}\delta_{ik}\hat{\partial}$	$-(\tilde{v}^c\rho_{ik}v+\tilde{w}^c\rho_{ik}w)$	$P_2(\boldsymbol{\sigma},\mathbf{n})$
2^{-+}	$^1D_2$	$(\overleftrightarrow{\partial}_i\partial_k-\frac{1}{3}\delta_{ik}(\partial)^2)\gamma_5$	$i(\tilde{v}^c\omega_{ik}w-\tilde{w}^c\omega_{ik}v)$	-
2^{--}	$^3D_2$	$(\gamma_i\partial_k+\gamma_k\partial_i-\frac{2}{3}\delta_{ik}\hat{\partial})\gamma_5$	$-(\tilde{v}^c\rho_{ik}w+\tilde{w}^c\rho_{ik}v)$	-
1^{--}	$^3D_1$	$\gamma_i\omega_{ik}$	$-(v^c\sigma_i\omega_{ik}v+\tilde{w}^c\sigma_i\omega_{ik}w)$	$\frac{3}{2}\sigma_i(n_i n_k-\frac{1}{3}\delta_{ik})$

$$\bar{y}_{123^*}=\frac{im_Q}{2\Omega^2\omega}\left(q_i(2\Omega+\omega)-\pi\frac{\omega\Omega}{\omega+\Omega}\right)\approx\frac{iq_i}{\omega}. \quad \text{(A6)}$$

We now turn to the case of (2×2) formalism, introduced in [17], where resulting kernels are denoted as $\bar{y}^{\rm red}_{123}$, and are computed according to

$$\bar{y}^{\rm red}_{123}={\rm tr}\{\Gamma^{(n_1)}_{\rm red}\Gamma^{(n_2)}_{\rm red}(\boldsymbol{\sigma}\mathbf{q})\Gamma^{(n_3)}_{\rm red}\}, \quad \text{(A7)}$$

while for emission of an additional pion in $\bar{y}^{(\pi){\rm red}}_{123}$ one should omit the factor $(\boldsymbol{\sigma}\mathbf{q})$ in (A7). In this way, one obtains $\Gamma_{\rm red}$ in Table II and (29) and (30). Note that normalization of states in (2×2) formalism is different, and one should sum up over all polarizations in initial and final states (the extra factor of $1/\sqrt{2}$ is in (A7) as compared to (A6), and $\frac{1}{\omega}\to\frac{1}{m+\varepsilon_n+\langle U\rangle-\langle V\rangle}$).

APPENDIX B: WAVE FUNCTIONS OF HEAVY QUARKONIA AND HEAVY-LIGHT MESONS

In Eq. (2) $R^{(n_1)}_{Q\bar{Q}}$, $R^{(n_2)}_{Q\bar{q}}$ and $R^{(n_3)}_{\bar{Q}q}$ are series of oscillator wave functions, which are fitted to realistic wave functions. We obtain them from the solution of the relativistic string Hamiltonian, described in [39].

In position space, the basic SHO radial wave function is given by

$$R^{\rm SHO}_{nl}(\beta,r)=\beta^{3/2}\sqrt{\frac{2(n-1)!}{\Gamma(n+l+1/2)}}(\beta r)^l e^{-\beta^2r^2/2}L^{l+1/2}_{n-1}(\beta^2r^2)$$
$$\int_0^\infty(R^{\rm SHO}_{nl}(\beta,r))^2r^2dr=1 \quad \text{(B1)}$$

where β is the SHO wave function parameter and $L^{l+1/2}_{n-1}(\beta^2r^2)$ is an associated Laguerre polynomial. The realistic radial wave function can be represented as an expansion in the full set of oscillator radial functions:

$$R_{nl}(r)=\sum_{k=1}^{k_{\rm max}}c_kR^{\rm SHO}_{kl}(\beta,r). \quad \text{(B2)}$$

Effective values of oscillator parameters β and coefficients c_k are obtained minimizing χ^2 and listed in the Table III.[2] In the momentum space, the SHO radial wave function is given by[3]

$$R^{\rm SHO}_{nl}(\beta,p)=\frac{(-1)^{n-1}(2\pi)^{3/2}}{\beta^{3/2}}\sqrt{\frac{2(n-1)!}{\Gamma(n+l+1/2)}}\left(\frac{p}{\beta}\right)^l e^{-p^2/2\beta^2}L^{l+1/2}_{n-1}\left(\frac{p^2}{\beta^2}\right)$$
$$\int_0^\infty\left(R^{\rm SHO}_{nl}(\beta,p)\right)^2\frac{p^2dp}{(2\pi)^3}=1. \quad \text{(B3)}$$

Then using Eq. (A16) from Appendix A of [25], one can write $I_{nn_2n_3}(\mathbf{p})$ in (32) from $n_2=n_3=1$ as ($\beta_1=\beta_{Q\bar{Q}}$, $\delta\beta_2=\beta_{Q\bar{q}}$)

$$I_{n11}(\mathbf{p})=\tilde{c}_n(-1)^{n-1}2\frac{(2n-1)!}{(n-1)!}\Phi\left(-(n-1),\frac{3}{2},\mathbf{f}^2\right)\times\frac{y^{n-1}}{(2\sqrt{\pi})^3}\left(\frac{2\beta_1^2\beta_2^2}{\Delta_n}\right)^{3/2} \quad \text{(B4)}$$

where

$$\Delta_n=2\beta_1^2+\beta_2^2,\qquad y=\frac{2\beta_1^2-\beta_2^2}{2\beta_1^2+\beta_2^2},\qquad \mathbf{f}=\frac{2\mathbf{p}\beta_1}{\Delta_n\sqrt{y}}, \quad \text{(B5)}$$

$$\tilde{c}_n=\left(\frac{2\pi}{\beta_1}\right)^{3/2}\frac{(2\sqrt{\pi}/\beta_2)^3}{\sqrt{2^{2n}\pi^{3/2}(2n-1)!}}. \quad \text{(B6)}$$

[2]Typos of the sign convection are corrected for the $1S$, $2S$, $3S$ charmonium states of [17]

[3]Note a typo in the equation for $R^{\rm SHO}_{nl}(\beta,p)$ of [17].

TABLE III. Effective values β (in GeV) and coefficients c_k of the series of oscillator radial wave functions $R_{kl}^{\mathrm{SHO}}(\beta, r)$ which are fitted to realistic radial wave functions $R_{nl}(r)$ of charmonium, bottomonium, B and D mesons.

State	β	c_1	c_2	c_3	c_4	c_5
			Bottomonium			
1S	1.27	0.977 164	−0.151 779	0.141 319	−0.020 857	0.036 863
2S	0.88	−0.188 23	0.953 901	−0.135 824	0.181 277	−0.001 509
3S	0.76	−0.128 081	−0.145 885	0.936 255	−0.169 962	0.226 281
4S	0.64	−0.019 432	−0.149 876	−0.362 548	0.88 647	0.014 308
5S	0.6	−0.011 183	−0.016 911	−0.182 019	−0.403 138	0.853 936
1P	0.93	0.977 994	−0.165 514	0.122 975	−0.018 631	0.024 364
2P	0.76	−0.092 083	0.971 982	−0.137 347	0.162 174	−0.002 707
1D	0.8	0.979 042	−0.168 619	0.11 132	−0.016 998	0.018 383
2D	0.69	−0.063 135	0.979 871	−0.117 356	0.145 358	0.000 973
			Charmonium			
1S	0.7	0.97 796	−0.169 169	0.117 682	−0.019 694	0.025 113
2S	0.53	−0.121 144	0.973 054	−0.130 808	0.141 495	0.00 097
3S	0.48	−0.096 897	−0.086 156	0.961 504	−0.155 931	0.178 935
4S	0.43	−0.021 639	−0.128 342	−0.215 657	0.947 215	−0.028 308
5S	0.41	−0.010 701	−0.022 826	−0.157 891	−0.258 875	0.925 921
1P	0.57	0.976 869	−0.184 163	0.105 506	−0.018 941	0.017 215
2P	0.48	−0.063 059	0.981 868	−0.123 012	0.127 035	0.000 588
1D	0.51	0.979 118	−0.178 313	0.095 356	−0.016 095	0.013 123
2D	0.45	−0.044 316	0.986 084	−0.107 408	0.117 002	0.001 907
			D meson			
1S	0.48	$c = 1$				
			B meson			
1S	0.49	$c = 1$				

Here, Φ is the confluent hypergeometric series,

$$\Phi(\alpha, \gamma, x) = 1 + \frac{\alpha}{\gamma 1!}x + \frac{\alpha(\alpha+1)}{\gamma(\gamma+1)2!}x^2 + \ldots$$

APPENDIX C: ANALYTIC STRUCTURE OF HADRON-QUARKONIUM RESONANCES

At the end, we study the analytic structure of the resonance denominator in $\frac{1}{1-\hat{K}\hat{\zeta}}$, which in the one-channel case is given by Eq. (55). One can write $K_n(E)$ as the integral

$$K_n(E) = \frac{1}{4\pi^2}\int_{m_\pi}^{\infty} d\omega\, \frac{k(\omega)\varphi^2(k)}{M_n + \omega - E}, \qquad \text{(C1)}$$

where $k(\omega) = \sqrt{\omega^2 - m_\pi^2}$. To display the analytic properties of $K_n(E)$, we shall use the method, exploited in [17], Appendix E, i.e. we replace the integral in (C1) as $1/2$ of the contour integral over the contour C, circumjacent to the interval $[m_\pi, \infty]$, as shown in Fig. 10, and take E in the physical region above the contour C, $E \to E + i\delta$, $\delta > 0$. Deforming the contour, so that it passes above and to the left of the point E (contour C' in Fig. 10), using Cauchy's theorem, one has the representation

$$K_n(E) = \frac{i}{4\pi}\varphi^2(k(E))k(E) + F_K(E) \equiv ia_K(E)k(E) + b_K(E). \qquad \text{(C2)}$$

Here, $k(E) = \sqrt{(E - M_n)^2 - m_\pi^2}$, and $F_K(E)$ is analytic function in the neighborhood of the threshold $E_{th}^{(n)} = M_n + m_\pi$. Hence $\mathrm{Re}[K_n(E)]$ acquires a negative contribution from the first term on the rhs of (C2) and behaves as shown in Fig. 10. This behavior of $\mathrm{Re}[K_n(E)]$ and $\mathrm{Im}[K_n(E)]$ agrees with that obtained by numerical integration in Fig. 6.

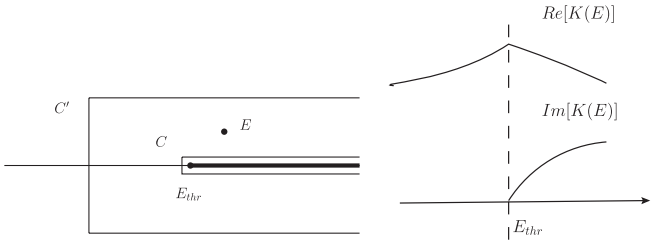

FIG. 10. a) Contours C and C' in the complex E plane, exibiting analytic properties of the integral (C4); b) Typical behavior of the $\mathrm{Re}[K_n(E)]$ and $\mathrm{Im}[K_n(E)]$ given by Eq. (C2).

In a similar way, one can write the form of $\zeta_{nm}(E)$

$$\zeta_{nm}(E) = \int_0^\infty \frac{pdp^2}{4\pi^2 N_c} \frac{\chi^2(p)}{(\frac{p^2}{2\tilde{M}} - z)}$$
$$= \frac{2\tilde{M}}{4\pi N_c}\{i\pi p(z)\chi^2(p(z)) + F_\zeta(z)\}$$
$$\equiv i a_\zeta(E) p(E) + b_\zeta(E), \quad \text{(C3)}$$

where $p(z) = \sqrt{2\tilde{M}z}$, $z = E - M_{n_2} - M_{n_3}$, $\tilde{M} = \frac{M_{n_2} M_{n_3}}{M_{n_2} + M_{n_3}}$, and a_i, $b_i (i = K, \zeta)$ are analytic and positive functions near the thresholds.

From (C2) and (C3), one can deduce that the product $K_n(E)\zeta_{nn}(E)$ is a real analytic function in the complex plane of E with cuts, starting at thresholds $E_{th}^{(n)} = M_n + m_\pi$ and $E_{n_2 n_3} = M_{n_2} + M_{n_3}$ and going to plus infinity. Thus, the combination $(1 - K_n(E)\zeta_{nn}(E))$ is a real analytic function in the E plane with positive weights in the integrals (C2) and (C3). Hence, the only possibility for the zeros of $(1 - K_n(E)\zeta_{nn}(E))$ is on the real axis below thresholds, or else on the next sheets, which implies a standard situation with possibility of bound state or virtual state poles, or else Breit-Wigner poles in $\frac{1}{1 - K_n(E)\zeta_{nn}(E)}$. From (C2) and (C3), one has

$$\frac{1}{1 - K_n(E)\zeta_{nn}(E)} = \frac{1}{1 - b_K b_\zeta + kpa_K a_\zeta - i(ka_K b_\zeta + pa_\zeta b_K)}. \quad \text{(C4)}$$

In the simple case, when the thresholds in $K_n(E)$ and $\zeta_{nn}(E)$ coincide, the resonance factor acquires the form

$$\frac{1}{1 - K_n(E)\zeta_{nn}(E)} = \frac{1}{A - ikB} \quad \text{(C5)}$$

with $B > 0$. This form demonstrates the appearance of a virtual ($A > 0$) or a real ($A < 0$) pole.

[1] S.-K. Choi *et al.* (Belle Collaboration), Phys. Rev. Lett. **94**, 182002 (2005); B. Aubert *et al.* (*BABAR* Collaboration), Phys. Rev. Lett. **101**, 082001 (2008); Phys. Rev. D **80**, 112002 (2009).
[2] S.-K. Choi, S. L. Olsen *et al.* (Belle Collaboration), Phys. Rev. Lett. **100**, 142001 (2008).
[3] R. Mizuk *et al.* (Belle Collaboration), Phys. Rev. D **78**, 072004 (2008); **80**, 031104(E) (2009).
[4] T. Aaltonen *et al.* (CDF Collaboration), Phys. Rev. Lett. **102**, 242002 (2009); arXiv:1101.6058.
[5] G. V. Pakhlova, arXiv:0810.4114; G. V. Pakhlova, P. N. Pakhlov, and S. I. Eidelman, Phys. Usp. **53**, 219 (2010); A. G. Mokhtar and S. L. Olsen, Chinese Phys. C **35**, 695 (2011).
[6] X. Liu, Y. R. Liu, W.-Z. Deng, and S. L. Zhu, Phys. Rev. D **77**, 034003 (2008).
[7] S. H. Lee, K. Morita, and M. Nielsen, Nucl. Phys. **A815**, 29 (2009).
[8] X.-H. Liu, Q. Zhao, and F. E. Close, Phys. Rev. D **77**, 094005 (2008).
[9] D. Dubynskiy and M. B. Voloshin, Phys. Lett. B **666**, 344 (2008).
[10] D. V. Bugg, J. Phys. G **35**, 075005 (2008).
[11] Youchang Yang, Zurong Xia, and Jialun Ping, Phys. Rev. D **81**, 094003 (2010).
[12] X. Liu, Z. G. Luo, Y. R. Liu, and S. L. Zhu, Eur. Phys. J. C **61**, 411 (2009).
[13] X. Liu and S. L. Zhu, Phys. Rev. D **80**, 017502 (2009).
[14] T. Branz, T. Gutsche, and V. E. Lyubovitskij, Phys. Rev. D **80**, 054019 (2009).
[15] Jian-Rong Zhang and Ming-Qiu Huang, Phys. Rev. D **80**, 056004 (2009); N. A. Tornqvist, Phys. Rev. Lett. **67**, 556 (1991); Z. Phys. C **61**, 525 (1994); X. Liu,Z.-G. Luo, and S. L. Zhu, Phys. Lett. B **699**, 341 (2011).
[16] Yan-Rui Liu and Zong-Ye Zhang, Phys. Rev. C **80**, 015208 (2009).
[17] I. V. Danilkin and Yu. A. Simonov, Phys. Rev. D **81**, 074027 (2010).
[18] I. V. Danilkin and Yu. A. Simonov, Phys. Rev. Lett. **105**, 102002 (2010).
[19] H. Y. Cheng, C. K. Chua, and A. Soni, Phys. Rev. D **71**, 014030 (2005).
[20] X. Liu, B. Zhang, and S. L. Zhu, Phys. Lett. B **645**, 185 (2007).
[21] C. Meng and K. T. Chao, Phys. Rev. D **75**, 114002 (2007).
[22] C. Meng and K. T. Chao, arXiv:0708.4222.
[23] C. Meng and K. T. Chao, Phys. Rev. D **77**, 074003 (2008).
[24] Yu. A. Simonov, Phys. At. Nucl. **71**, 1048 (2008).
[25] Yu. A. Simonov and A. I. Veselov, Phys. Rev. D **79**, 034024 (2009).
[26] Yu. A. Simonov and A. I. Veselov, Phys. Lett. B **671**, 55 (2009); **673**, 211(E) (2009).
[27] Yu. A. Simonov and A. I. Veselov, JETP Lett. **88**, 5 (2008).
[28] Yu. A. Simonov, Phys. Rev. D **84**, 065013 (2011).
[29] A. M. Badalian, L. P. Kok, M. I. Polikarpov, and Yu. A. Simonov, Phys. Rep. **82**, 31 (1982).
[30] K. Abe *et al.* (Belle Collaboration), arXiv:hep-ex/0505037.
[31] D. Liventsev (for Belle Collaboration), arXiv:1105.4760.

[32] E. van Beveren and G. Rupp, Ann. Phys. (N.Y.) **324**, 1620 (2009);
[33] S. Coito, G. Rupp, and E. van Beveren, Eur. Phys. J. C **71**, 1762 (2011).
[34] P. Geiger and N. Isgur, Phys. Rev. D **41**, 1595 (1990).
[35] N. Cardoso, M. Cardoso, and P. Bicudo, arXiv:1108.1542.
[36] P. S. Kuzmenko, V. I. Shevchenko, and Yu. A. Simonov, Phys. Usp. **174**, 3 (2004), 10.3367/UFNr.0174.200401a.0003.
[37] I. Adachi *et al.* (Belle Collaboration), arXiv:1105.4583.
[38] Y. A. Simonov, J. A. Tjon, and J. Weda, Phys. Rev. D **65**, 094013 (2002).
[39] A. M. Badalian, A. I. Veselov and B. L. G. Bakker, J. Phys. G **31**, 417 (2005); A. M. Badalian and I. V. Danilkin, Phys. At. Nucl. **72**, 1206 (2009); A. M. Badalian, B. L. G. Bakker, and I. V. Danilkin, Phys. At. Nucl. **72**, 638 (2009); Phys. Rev. D **79**, 037505 (2009); A. M. Badalian and B. L. G. Bakker, Phys. Lett. B **646**, 29 (2007); Phys. At. Nucl. **70**, 1764 (2007); A. M. Badalian and I. V. Danilkin, Phys. At. Nucl. **72**, 1206 (2009).
[40] A. E. Bondar, A. Garmash, A. I. Milstein, R. Mizuk, and M. B. Voloshin, Phys. Rev. D **84**, 054010 (2011).
[41] P. Pakhlov, Phys. Lett. B **702**, 139 (2011).
[42] Jian-Rong Zhang, Ming Zhong, and Ming-Qiu Huang, Phys. Lett. B **704**, 312 (2011).
[43] D. V. Bugg, Europhys. Lett. **96**, 11002 (2011).
[44] Dian-Yong Chen, Xiang Liu, and Shi-Lin Zhu, Phys. Rev. D **84**, 074016 (2011).